Ab initio Study on Luminescence and Aurophilicity of a Dinuclear $[(AuPH_3)_2(i\text{-}mnt)]$ Complex (i-mnt = isomer-Malononitriledithiolate)

Qing-Jiang Pan,[a,b] and Hong-Xing Zhang*[a]

Keywords: Ab initio calculations / Luminescence / Aurophilicity / Excited state

The luminescence and Au–Au aurophilicity of the model complex, $[(AuPH_3)_2(i\text{-}mnt)]$ (i-mnt = isomer-malononitriledithiolate in both solid state and solution have been studied by ab initio methods. The structures of the Au^I complex were fully optimized by the MP2 method for the ground state and the CIS method for the excited state. The b^3A' excited-state Au–Au (2.946 Å) and the corresponding Au–Au stretching frequency (83 cm^{-1}) indicate intramolecular Au–Au aurophilicity. Using $[(AuPH_3)_2(i\text{-}mnt)]_2$ to rationalize the solid-state emission to the $[(AuPPh_3)_2(i\text{-}mnt)]$ complex at 20 K we assigned the experimental emission (462 nm) to an Au–Au→i-mnt charge-transfer (^{3}MMLCT) transition from the triplet excited state to the ground state. In the ^{3}MMLCT emissive excited state, the Au–Au aurophilicity, including intra- and intermolecular Au–Au interactions, results in a ca. 120 nm red shift in emission relative to that of mononuclear PH_3AuSH. The calculated absorption and emission in dichloromethane solution agree with the experimental results. These results, combined with our previous studies on both $[Au_2(dpm)_2]^{2+}$ [dpm = bis(diphosphanyl)methane] and $[Au_2(dpm)(i\text{-}mnt)]$, indicate a clear correlation between Au–Au aurophilicity and the excited-state properties of the dinuclear Au^I complexes.

Introduction

The luminescence and aurophilicity of Au^I complexes have been extensively studied over the last two decades.[1−10] Many Au^I complexes luminesce in the solid state and/or in solution, mostly accompanied by intra- and/or intermolecular Au−Au interactions.[11−18] By experiments and accurate theoretical calculations containing electron correlation and relativistic effects, the energy of the Au−Au attraction was estimated to be 5−15 kcal/mol, similar to that of hydrogen bonds.[19−23] The photoluminescence properties of di- and polynuclear Au^I complexes are highly diversified. For various bridging and ancillary ligands, the luminescence properties of such complexes have been suggested to range from MLCT (metal-to-ligand charge transfer), LMCT (ligand-to-metal charge transfer), MCCT (metal-centered charge transfer) and ILCT (intraligand charge transfer).[24−27]

The Au−Au aurophilicity is correlated with the excited-state properties, especially for MCCT in dinuclear Au^I complexes such as those with bridging phosphane ligands, which possess a lower-energy phosphorescence (500−600 nm) in acetonitrile.[26,27] Ab initio calculations indicated that the $^3(d_{\sigma^*}s_\sigma)$ excited state corresponding to the lower-energy emission presents an Au−Au distance of ca. 2.72 Å, which is much shorter than the ca. 3.16 Å in the ground state.[28] The promotion of electron from the d_{σ^*} antibonding orbital to the s_σ bonding orbital affords an Au−Au σ single bond in the MCCT emissive excited state. In addition, for the well-known dinuclear Pt^{II} complex $[Pt_2(pop)_4]^{4-}$ (pop = pyrophosphate), Pt−Pt in the $^3(d_{\sigma^*}p_\sigma)$ excited state shortens by ca. 0.29 Å relative to that in the ground state, which is supported by both the excited-state structure from time-resolved X-ray diffraction and ab initio studies.[29,30]

For Au^I complexes containing both phosphane and thiolate ligands, the lower-energy emissions in the solid state have been experimentally attributed to Au→thiolate charge transfer (MLCT).[11,17,24,31−36] Bruce's studies on a series of dinuclear (phosphane)Au^I thiolates with or without Au−Au interaction showed that the interaction is not a necessary condition for luminescence and that its presence does not significantly perturb the luminescence;[32] however, Fackler and co-workers found that the emission maximum in the luminescence of many mononuclear (phosphane)Au^I thiolate complexes can be affected by an Au−Au interaction.[11] In fact, such studies are not incompatible. The charge transfer from metal to ligand should be divided into metal−metal-to-ligand charge transfer (MMLCT) and metal-to-ligand charge transfer (MLCT).[12,18,37] The former is clearly correlated with the Au−Au interaction but the latter does not.

[a] State Key Lab of Theoretical and Computational Chemistry, Institute of Theoretical Chemistry, Jilin University, Changchun 130023, P. R. China
Fax: (internat.) + 86-431/8945942
E-mail: hxzhang@mail.jlu.edu.cn
[b] College of Chemistry and Chemical Engineering, Heilongjiang University, HaerBin 150080, China

  DOI: 10.1002/ejic.200300389

Unlike those of dinuclear Au^I complexes with bridging phosphane ligands, the excited-state properties of dinuclear (phosphane)Au^I thiolates are clearly related to MMLCT or MLCT, in which the thiolate ligands are greatly involved in the luminescence.[31−36] This is because phosphane ligands always provide lone-pair electrons to form the dative P→Au bond while thiolates, usually as anions, prefer the covalent S−Au bond to coordinating. These different electronic properties may lead to differences in luminescence and aurophilicity when thiolates are introduced into (phosphane)Au^I complexes to form (phosphane)Au^I thiolate complexes.

To study both their luminescent properties and Au−Au aurophilicity, several dinuclear Au^I complexes have been designed, with at least two different structural arrangements: the more common dinuclear Au^I dimers, in which the aurophilicity is sterically imposed,[26,27,38,39] and the open-ring structural disposition, in which the interaction between two Au^I atoms, if it appears, is not sterically imposed.[31−34,40,41] The structurally characterized (phosphane)Au^I thiolate [$(AuPPh_3)_2$(i-mnt)] (i-mnt = isomer-malononitriledithiolate has a nonimposed intramolecular Au−Au interaction.[41] The intense 462 nm phosphorescence of the solid-state complex at 20 K was assigned as an Au→thiolate charge transfer (^{3}MLCT) from the triplet excited state to the ground state.[33,34] Since the π-conjugated i-mnt ligand is greatly involved in the emission and Au−Au aurophilicity is possibly present in the corresponding excited state, the [$(AuPPh_3)_2$(i-mnt)] complex may be an ideal candidate for the ^{3}MMLCT emissive excited state.

Dinuclear Au^I thiolates have also been widely applied in medicine,[42] optical sensors,[12,13,43] and photoredox chemistry.[22,24,27,44] For example, the therapeutic action of gold drugs for rheumatoid arthritis may be related to the ability of the Au^I complexes to quench the singlet oxygen $^1\Delta_g$ state at 7752 cm^{-1}.[42c] Eisenberg and co-workers have reported that [Au{$S_2CN(C_5H_{11})_2$}]$_2$ can be used to monitor efficiently volatile organic compounds (VOCs), by a reversible interaction with VOC vapors that results in both a dramatic color change and a positive "switching on" of luminescence.[13] Such applications make use of excited-state properties. Thus, theoretical investigation of the electronic structures of the ground and excited states for the Au^I complexes is also of practical significance.

Here, ab initio methods have been employed to study the spectroscopic properties and Au−Au aurophilicity of [$(AuPH_3)_2$(i-mnt)] in both solid state and solution. In the solid state, the calculated 450-nm phosphorescence of [$(AuPH_3)_2$(i-mnt)]$_2$ was assigned as an Au−Au→i-mnt charge transfer (^{3}MMLCT) from the triplet excited state to the ground state, similar to the 462-nm solid-state emission of the [$(AuPPh_3)_2$(i-mnt)] complex at 20 K. In the ^{3}MMLCT emissive excited state of polynuclear [$(AuPH_3)_2$(i-mnt)]$_2$, both intra- and intermolecular Au−Au interactions strongly affect the solid-state emission, causing a ca. 120 nm red shift with respect to the 332-nm emission of mononuclear PH_3AuSH. The studies of $[Au_2(dpm)_2]^{2+}$ [dpm = bis(diphosphanyl)methane],[28] [$(AuPH_3)_2$(i-mnt)] and [Au_2(dpm)(i-mnt)] show that the Au−Au aurophilicity is clearly correlated with the excited-state properties of these Au^I complexes.

Computational Details and Theory

In the calculations, [$(AuPH_3)_2$(i-mnt)] was employed to represent the real [$(AuPPh_3)_2$(i-mnt)] complex. A similar model was applied in our previous work[28] by using dpm to stand for dmpm, dppm and dcpm in the $[Au_2(dmpm)_2]^{2+}$, $[Au_2(dppm)_2]^{2+}$ and $[Au_2(dcpm)_2]^{2+}$ complexes respectively [dmpm = bis(dimethylphosphanyl)methane, dppm = bis(diphenylphosphanyl)methane and dcpm = bis(dicyclohexylphosphanyl)methane]. Hydrogen is generally used in place of methyl, phenyl substituents etc. in ab initio studies to save computational resources. Häberlen and Rösch[45] have proved that PH_3 provided a satisfactory model for PMe_3 or PPh_3 for the structural properties of Au^I complexes. Bruce[22] and other researchers[26,46,47] have successfully used such a kind of model in their theoretical studies on the related topics of (phosphane)Au^I complexes.

Here, the C_s symmetry was adopted to settle the conformation of [$(AuPH_3)_2$(i-mnt)] in both the ground and excited states. The structures of the ground and excited states were fully optimized by the second-order Møller−Plesset perturbation (MP2)[48] and the single excitation configuration interaction (CIS)[49] methods, respectively, in which electron correlation effects were considered.[22,23] Based on such calculations, the isodensity-polarized continuum model (IPCM) in the self-consistent reaction field (SCRF) method[50−53] was employed to account for the solvent effect of dichloromethane, by considering the dramatic red shift of emission due to the solvation of acetonitrile on $[Au_2(dpm)_2]^{2+}$ indicated previously.[28] Therefore, the electronic structure of the excited state and the absorption and emission in CH_2Cl_2 solution were obtained.

In the calculations, the quasi-relativistic pseudopotentials of the Au, S and P atoms proposed by Hay and Wadt[54] with 19, 6 and 5 valence electrons, respectively, were employed and the LANL2DZ basis sets associated with the pseudopotential were adopted and implemented by one additional f-type function for Au (α_f = 0.2), and a d-type function for S (α_d = 0.421) and P (α_d = 0.34).[23] The basis sets were taken as Au(8s6p3d1f/3s3p2d1f), S(3s3p1d/2s2p1d), P(3s3p1d/2s2p1d), N(10s5p/3s2p), C(10s5p/3s2p) and H(4s/2s). Thus, 176 basis functions and 104 electrons were included for [$(AuPH_3)_2$(i-mnt)] in the calculations. All the calculations were performed with the Gaussian98 program package[53] using an Origin/3800 server.

Result and Discussion

A. Structures of the Ground and Excited States of [$(AuPH_3)_2$(i-mnt)]

The full MP2 optimizations on [$(AuPH_3)_2$(i-mnt)] indicate that the complex has a $^1A'$ ground state with [(28a′^{2})-

Table 1. Optimized geometry parameters of the $^1A'$ ground state using the MP2 method and the a^3A' and b^3A' excited states using the CIS method for $[(AuPH_3)_2(i\text{-}mnt)]$, together with the experimental data of $[(AuPPh_3)_2(i\text{-}mnt)]$

Parameters	Ground state $^1A'$	Experiment	Excited state a^3A'	b^3A'
Bond lengths [Å]:				
Au1−Au2	2.945	3.156	4.753	2.946
Au1−P3	2.327	2.257	2.390	2.477
Au1−S5	2.335	2.313	2.380	2.506
S5−C7	1.782	1.729	1.771	1.740
C7−C8	1.406	1.372	1.490	1.402
C8−C9	1.455	1.432	1.423	1.434
C9−N11	1.216	1.132	1.158	1.154
P3···P4	3.826		6.657	5.966
S5···S6	3.223		3.108	3.152
Bond angles [°]:				
P3−Au1−S5	165.7	172.1	176.7	140.1
P3−Au1−Au2	100.9		113.5	127.6
S5−Au1−Au2	93.4		69.8	92.4
S5−C7−S6	129.4	123.2	122.6	129.9
Dihedral angles [°]:				
P3−Au1−Au2−S6	180.0		179.4	−179.8
S5−C7−C8−S6	−179.4		176.2	−180.0
Au1−S5−S6−C7	−178.1		−87.9	−179.9

$(24a''^2)$] electronic configuration. The calculated main geometry parameters are listed in Table 1, associated with the data from X-ray crystal diffraction for the $[(AuPPh_3)_2(i\text{-}mnt)]$ complex.[41] The structure of the $^1A'$ ground state (Figure 1, a) consists of two $AuPH_3$ units bridged by an i-mnt ligand. The calculated dihedral angles of 180.0° (P3−Au1−Au2−S6), −179.4° (S5−C7−C8−S6) and −178.1° (Au1−S5−S6−C7) indicate that the molecule is nearly coplanar. The Au^I atom has a linear two-coordinate structure with a P3−Au1−S5 angle of 165.7°, which is similar to the experimental 172.1°. The calculated Au−Au (2.945 Å) bond is shorter than the 3.156 Å determined by experiment for $[(AuPPh_3)_2(i\text{-}mnt)]$ (Table 1) because we used the hydrogen atom in place of the phenyl ligand on the P atoms − the bulky phenyl ligand does not facilitate the approach of two Au^I atoms. Bruce et al.[22] have studied theoretically the luminescent properties and Au−Au aurophilicity of *cis*- and *trans*-$[Au_2X_2CH_2(PH_2)_2]$ (X = Cl, Br and I) complexes, in which the same approximation was employed. Their calculated results agreed well with experimental observations and revealed the nature of the excited states of the real $[Au_2X_2CH_2(PPh_2)_2]$ complex. Thus, our approximation applied here may have little effect on the excited-state properties of the $[(AuPPh_3)_2(i\text{-}mnt)]$ complex. The other distances in the $^1A'$ ground state presented by MP2 calculations accord with those determined experimentally (Table 1).

The frequencies calculated for the ground state of $[(AuPH_3)_2(i\text{-}mnt)]$, performed at the MP2 level, are all low relative to experiment (Table 2), but parallel them because of the ratio of calculation to experiment of 0.80−0.84, excluding the C=C stretching vibration. The 42 cm^{-1} frequency was assigned as the Au−Au stretching vibration and fell

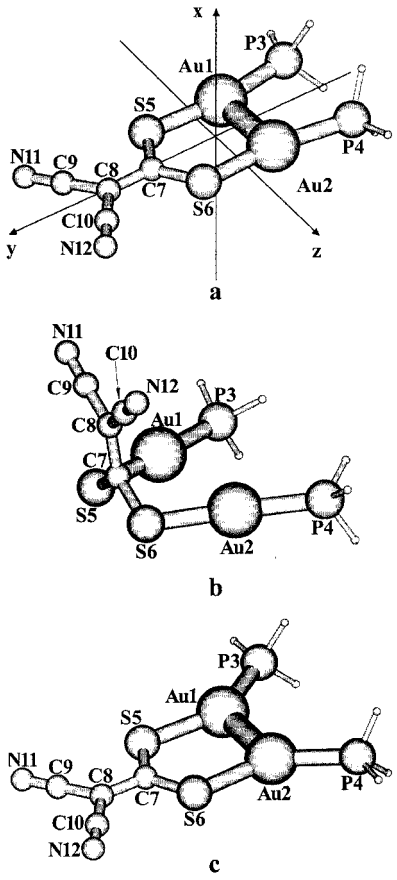

Figure 1. Optimized $^1A'$ (a) ground-state structure using the MP2 method, and the optimized a^3A' (b) and b^3A' (c) excited-state structures using the CIS method for $[(AuPH_3)_2(i\text{-}mnt)]$

Table 2. Calculated frequencies at the MP2 level for the $^1A'$ ground state of $[(AuPH_3)_2(i\text{-}mnt)]$, associated with Raman frequencies of $[(AuPPh_3)_2(i\text{-}mnt)]$

Assignment	Frequencies [cm^{-1}] Calcd.	Exp.	Calcd./exp.
ν(Au-Au)	42	36−71[a]	
ν(Au−P)	324	385	0.8416
ν(Au−S)	396	480	0.8250
ν(C−S)	695	865	0.8035
ν(C=C)	1372	1410	0.9730
ν(C≡N)	1856	2209	0.8402

[a] Frequencies of ν(Au−Au) from ref.[55]

well within the experimental range reported for such vibrations,[55] suggesting weak aurophilicity between the two Au^I atoms in the $^1A'$ ground state.

The CIS method was used to optimize the structure of the excited state of $[(AuPH_3)_2(i\text{-}mnt)]$. Two triplet excited states were obtained with a^3A' and b^3A' symmetries. The calculated geometry parameters (Table 1) and the corresponding structures (Figure 1, b and c) are given here. Apparently, the geometry of the excited states changes greatly with respect to that of the ground state. In the a^3A' excited state the i-mnt ligand deviates from the $Au_2S_2P_2$ plane due to the dihedral angle of −87.9° for Au1−S5−S6−C7, and

almost all the ligand bonds are longer than those in the $^1A'$ ground state (Table 1). The two Au atoms are much farther apart (4.753 Å) than in the $^1A'$ ground state (2.945 Å), suggesting no Au−Au aurophilicity as the separation is much more than the van der Waals contact (3.4 Å).[56] Thus, the a^3A' excited state may be related to i-mnt intraligand charge-transfer character.

Unlike the a^3A' excited state, the geometry of the b^3A' excited state is still in a plane, which is intuitively depicted in Figure 1 (c) and quantitatively reflected in Table 1. The Au−Au (2.946 Å) is close to that in the $^1A'$ ground state, but the P···P distance (5.966 Å) in the excited state is far longer than the 3.826 Å in the ground state. This implies a significant Au−Au aurophilicity in the b^3A' excited state as the two P atoms tend to separate in opposite directions. To characterize the Au−Au interaction in the b^3A' excited state of $[(AuPH_3)_2$(i-mnt)], we also carried out frequency calculations. Through vibrational-mode analysis, the calculated frequency of 83 cm^{-1} was attributed to the Au−Au stretching frequency in the excited state, which is much higher than the 42 cm^{-1} frequency in the $^1A'$ ground state. The Au−Au stretching frequency provides evidence of aurophilic attraction between the two gold atoms in both the b^3A' excited state and the $^1A'$ ground state. In addition, the calculated overlap population between the two Au atoms is 0.062 and 0.036 for the b^3A' excited state and $^1A'$ ground state respectively. From such calculated frequencies and overlap populations between the two Au atoms, it is easily seen that although the Au−Au distances are very close in the b^3A' excited state (2.946 Å) and the $^1A'$ ground state (2.945 Å), the Au−Au aurophilicity in the former is stronger. This suggests that there may be some electron transfer to the 6s and/or 6p bonding orbitals of Au atoms in the b^3A' excited state, which then reinforces the Au−Au interaction.

B. Absorption Spectra of $[(AuPH_3)_2$(i-mnt)] in the CH_2Cl_2 Solution

Keeping the optimized structure of the ground state constant, the CIS method was used to calculate the excited state related to absorption. Based on such calculations, the solvent effect of dichloromethane was taken into account by the IPCM in the SCRF method[50−53] and absorption spectra of $[(AuPH_3)_2$(i-mnt)] in solution were obtained. The calculated absorption and the corresponding oscillator strength are given in Table 3, together with the experimental results of $[(AuPPh_3)_2$(i-mnt)] available in the CH_2Cl_2 solution at room temperature.

To assign the absorption in solution, the partial molecular orbital compositions (%) involved in the absorption transition are listed in Table 4, associated with the orbital components. The coordinate orientation of $[(AuPH_3)_2$(i-mnt)] is depicted in Figure 1 (a), in which the z axis parallels the line through the two Au atoms.

The calculated absorption maximum in CH_2Cl_2 solution is at 303 nm with the nature of an $X^1A'\rightarrow A^1A''$ transition. In the excitation, the $24a''\rightarrow 29a'$ configuration has the largest coefficient (ca. 0.6) in the CI wavefunctions, and is responsible for the absorption. The 24a′′ orbital (HOMO-1) has 68% i-mnt ligand composition, mainly contributed by the $S(p_y)$ orbital, while the metal (62%) plays an important role in the 29a′ orbital (LUMO), mainly from the $Au(p_z)$ character (Table 4). Thus, the 303-nm absorption, arising from the $X^1A'\rightarrow A^1A''$ transition, is attributed to $S(p_y)\rightarrow Au(p_z)$ charge transfer (LMCT) mixed with some $Au(d_{z^2})\rightarrow Au(p_z)$ charge transfer (MCCT), which corresponds to the 365-nm absorption observed experimentally for $[(AuPPh_3)_2$(i-mnt)] at room temperature.[33] The large difference between calculated and experimental absorption wavelength is caused mainly by the use of a hydrogen atom to represent the bulky phenyl ligand on P atoms. In a real $[(AuPPh_3)_2$(i-mnt)] system, the relatively longer Au−Au distance may result in less metal participation in the 24a′′ (HOMO-1) orbital. Because the order of the energy level in occupied orbitals is $S(p_\pi) > Au(d_{\sigma^*})$ by analyzing the wavefunctions, the lesser Au contribution to the transition wound reduce the excitation energy. Therefore, if the steric bulk of the phenyl ligands on P atoms was taken into account, the calculated absorption maximum would red-shift relative to the 303 nm of $[(AuPH_3)_2$(i-mnt)] and approach the experimental value of 365 nm.

For the B^1A' excited state, the corresponding absorption was calculated at 295 nm with an oscillator strength of 0.765, which is similar to the 310-nm absorption of the experiment[33] (Table 3). The transition arises mainly from the $28a'\rightarrow 30a'$ configuration with the largest CI coefficient of ca. −0.6. From Table 4, the 295 nm absorption from an $X^1A'\rightarrow B^1A'$ transition was assigned as i-mnt intraligand charge transfer (ILCT) with some LMCT. Because the B^1A' excited state has ILCT character and less metal participation, the approximation overestimating the metal−metal interaction does not significantly perturb the absorption, i.e. the calculated absorption wavelength of 295 nm agrees with the experimental absorption (310 nm).[33] To intuitively understand the absorption process, the density diagrams of the frontier molecular orbitals are depicted in Figure 2. In the 28a′ orbital (HOMO) the electron density mainly focuses around the i-mnt ligand, with the C7−C8 π-bonding orbitals, while in the 30a′ (LUMO+1) and 31a′ (LUMO+3) orbitals the electron density is still distributed on the i-mnt ligand and π* antibonding orbitals form between the two carbon atoms. Thus, we can further assign the 295-nm absorption to a $\pi\rightarrow\pi^*$ transition involving the C=C double bond. Gray et al.[57] have studied the electronic spectra of a series of metal complexes containing the i-mnt ligand in acetonitrile and attributed the absorptions in the range 250−350 nm to $L\rightarrow L^*$ charge transfer.

As a reference, the same methods and basis sets as those of $[(AuPH_3)_2$(i-mnt)] were used to calculate electronic spectra of the organic i-mnt ligand. The ligand also has a C_s symmetry in the calculations of both ground and excited states. The calculated absorption maximum in CH_2Cl_2 solution of 268 nm (Table 3), arising from a $\pi\rightarrow\pi^*$ transition localized on the C=C double bond, supports our assignment for the 295 nm absorption of $[(AuPH_3)_2$(i-mnt)].

Table 3. Calculated absorption and emission of $[(AuPH_3)_2(i\text{-mnt})]$ and i-mnt ligand in the solid state and CH_2Cl_2 solution under the CIS calculations, together with experimental results

		Solid state Calcd. [nm]	Exp. [nm]	CH_2Cl_2 solution Calcd. [nm]	Exp. [nm]
$[(AuPH_3)_2(i\text{-mnt})]$	absorption			303 (0.068)[a]	365[b]
				295 (0.765)[a]	310[b]
				238 (0.364)[a]	225[b]
	emission	593	595[c]	702	
		414/450[d]	462[e]	333	
i-mnt ligand	absorption			268 (0.512)[a]	275[f]
	emission	611	595[c]	714	

[a] Oscillator strength in parentheses. [b] Absorptions of $[(AuPPh_3)_2(i\text{-mnt})]$ in CH_2Cl_2 solution at room temperature from ref.[33] [c] Solid-state emission of $K_2(i\text{-mnt})$ at 20 K from refs.[33,34] [d] 414- and 450-nm emissions from $[(AuPH_3)_2(i\text{-mnt})]$ and $[(AuPH_3)_2(i\text{-mnt})]_2$, respectively, from the present work. [e] Solid-state emission of $[(AuPPh_3)_2(i\text{-mnt})]$ at 20 K from ref.[33] [f] Average value of absorptions of a series of metal complexes with the i-mnt ligand in acetonitrile from ref.[57]

Table 4. Partial molecular orbital compositions (%) of $[(AuPH_3)_2(i\text{-mnt})]$ in CH_2Cl_2 solution under the CIS calculations

MO	Energy [eV]	Composition (%) 2 Au	i-mnt	2 PH_3	Components of orbital
34a′	3.1563	54.7	0.6	44.6	$Au(p_x) + P(p_x)$
33a′	2.8292	69.1	25.8	5.1	$Au(p_y) + S(p_y) + C7(p_y) + C8(p_y)$
32a′	2.2251	59.7	7.6	32.7	$Au(p_z) + P(p_z)$
26a"	1.9171	78.3	18.7	3.0	$Au(s,p_z)$
31a′	1.7527	15.2	72.1	12.7	$S(p_x) + C7(p_x) + Au(p_x)$
25a"	1.6085	75.4	4.6	20.0	$Au(p_x)$
30a′	0.1195	27.8	54.1	18.2	$C7(p_x) + C8(p_x) + N11(p_x) + Au(p_x)$
29a′ (LUMO)	0.0656	62.1	18.7	19.2	$Au(p_z)$
28a′ (HOMO)	−8.2323	5.5	94.1	0.4	$S(p_x) + C8(p_x) + N11(p_x)$
24a"	−8.6168	24.4	68.4	7.2	$S(p_y) + Au(d_{z^2})$
23a"	−9.0136	12.0	87.4	0.7	$S(p_x)$
22a"	−10.1012	40.2	14.8	45.0	$Au(d_{xy},p_y) + P(p_y)$
27a′	−10.3045	16.4	79.1	4.6	$S(p_y)$
26a′	−11.9418	44.1	17.9	37.9	$Au(d_{x^2-y^2},s) + P(p_y)$
25a′	−12.2743	8.8	90.5	0.7	$C7(p_x) + C9(p_x) + N11(p_x) + S(p_x)$
21a"	−12.3432	8.9	89.9	1.2	$S(p_y) + N7(p_y) + C9(p_y) + N11(p_y)$

The calculated 238-nm absorption from $X^1A' \rightarrow C^1A''$ is related to charge transfer between Au atoms and phosphane ligands. The main configuration 22a′′→29a′, gives rise to the absorption. The 22a′′ orbital has 45% PH_3 and 40% Au orbital character. Therefore, the 238-nm absorption was assigned as $P(p_y) \rightarrow Au(p_z)$ charge transfer (LMCT) mixed with MCCT transitions, which is similar to the observed 225-nm absorption.[33]

C. Emission Spectra of $[(AuPH_3)_2(i\text{-mnt})]$ in the Solid State and CH_2Cl_2 Solution

The excited-state structure was fully optimized by the CIS method to describe the emissive properties of $[(AuPH_3)_2(i\text{-mnt})]$. Two triplet a^3A' and b^3A' excited states were obtained in the CIS calculations and the corresponding emissions were at 593 and 414 nm, respectively, for a single $[(AuPH_3)_2(i\text{-mnt})]$ molecule (Table 3).

By analyzing the wavefunctions of the a^3A' excited state, the calculated 593-nm emission was assigned as a $\pi^* \rightarrow \pi$ charge transfer (i-mnt ^{3}ILCT) involved in the C=C double bond from the triplet excited state to the $^1A'$ ground state, similar to the 595-nm emission of $K_2(i\text{-mnt})$ in the solid state at 20 K.[33] The $\pi^* \rightarrow \pi$ transition is reflected in the structural change of the a^3A' excited state (Table 1). The calculated C7=C8 distance (1.490 Å) in the excited state is longer than that in the $^1A'$ ground state (1.406 Å), suggesting a π^*-orbital character between the two carbon atoms in the excited state. By the combination of the CIS method and the IPCM in the SCRF method, the $[(AuPH_3)_2(i\text{-mnt})]$ complex has a 702-nm emission in the CH_2Cl_2 solution. The solvent effect results in a red shift of ca. 110 nm relative to the emission in the solid state (593 nm). Using the same methods, the lowest-energy emission of the organic i-mnt ligand was calculated at 611 nm, originating from a $^3A' \rightarrow {}^1A'$ transition in the solid state, and at 714 nm in CH_2Cl_2 solution (Table 3), which supports our assignment for such emissions of $[(AuPH_3)_2(i\text{-mnt})]$.

With respect to the $b^3A' \rightarrow {}^1A'$ transition, the corresponding emission is calculated at 414 nm for the single $[(AuPH_3)_2(i\text{-mnt})]$ molecule. To characterize the emission process, we used the difference in the natural atomic orbital populations for the b^3A' excited state and the correspond-

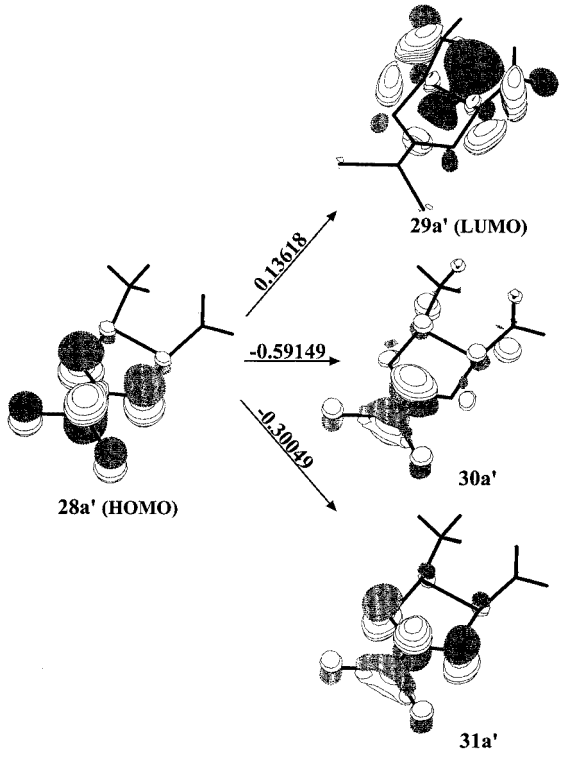

Figure 2. Single-electron transitions with (CI coefficient) > 0.1 in the CIS calculations for the 295 nm absorption of $[(AuPH_3)_2$(i-mnt)] in CH_2Cl_2 solution

Table 5. Natural atomic orbital populations of the b^3A' excited state and the corresponding $^1A'$ ground state for the 414 nm emission of $[(AuPH_3)_2$(i-mnt)] under the CIS calculations

	Atom	Orbital	$^1A'$	b^3A'
	Au	6s	0.647	0.889
		6p	0.024	0.080
		5d	9.863	9.860
		4f	0.003	0.004
i-mnt ligand	S	3s	1.711	1.713
		3p	4.563	4.383
		3d	0.025	0.025
	C7	2s	1.055	1.079
		2p	3.128	3.155
	C8	2s	0.902	0.904
		2p	3.490	3.165
	C9	2s	0.845	0.851
		2p	2.799	2.818
	N11	2s	1.594	1.595
		2p	3.814	3.743
PH_3 ligand	P	3s	1.418	1.433
		3p	3.332	3.374
		3d	0.055	0.055
	H_{P1}	1s	0.990	1.003
	H_{P2}	1s	1.014	1.012

ing $^1A'$ ground state for $[(AuPH_3)_2$(i-mnt)] (Table 5). The electron transition is dominated by the metal centers and the i-mnt ligand (Table 5), while the charge transfer localized on the PH_3 ligand changes little. There are ca. 0.59 electrons to transfer from two Au atoms to the i-mnt ligand in the emissive process, in which 6s and 6p orbitals of Au

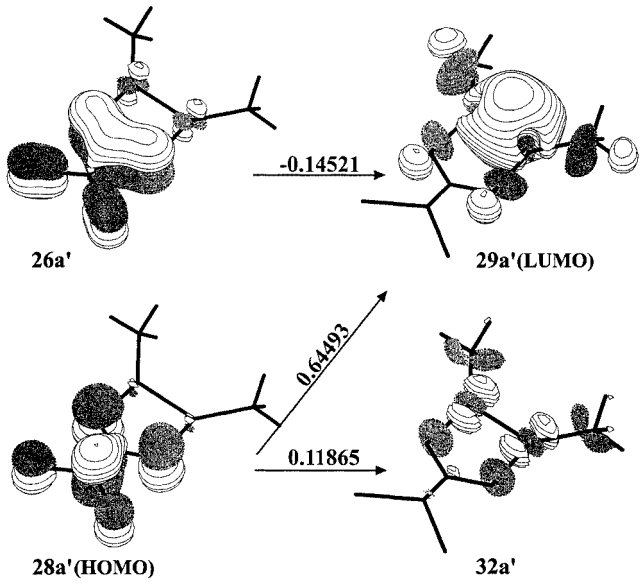

Figure 3. Single-electron transitions with (CI coefficient) > 0.1 in the CIS calculations for the 414-nm phosphorescence of $[(AuPH_3)_2$(i-mnt)]

atom lose ca. 0.24 and 0.06 electrons, respectively, and the $3p_x$ orbital of the S atom and the $2p_x$ orbital of the C8 atom increase by ca. 0.18 and 0.32 electrons, respectively. Therefore, we attributed the 414-nm emission to an Au→i-mnt charge transfer (^{3}MLCT) from the triplet b^3A' excited state to the $^1A'$ ground state. Density diagrams of the frontier molecular orbitals (Figure 3) help us intuitively understand the transition process. In the 26a′ and 28a′ orbitals, the electron density mainly focuses around the i-mnt ligand while the electron density transfers to Au centers to form a σ-bonding orbital in 29a′. Electron promotion from the i-mnt ligand orbitals to s_σ and p_σ orbitals of the Au atoms results in an Au−Au σ bond in the b^3A' excited state. The density diagrams seem to show significant Au−Au aurophilicity in the excited state, and that the Au−Au aurophilicity is relatively stronger in the b^3A' excited state than in the $^1A'$ ground state. Therefore, the 414-nm emission corresponding to the b^3A' excited state should have Au−Au→i-mnt charge transfer (^{3}MMLCT) character.

To reveal the effect of Au−Au aurophilicity on the luminescence in the b^3A' excited state of a $[(AuPH_3)_2$(i-mnt)] molecule, the mononuclear PH_3AuSH molecule was calculated using the same methods and basis sets as those of the dinuclear $[(AuPH_3)_2$(i-mnt)] complex. The 332-nm emission of PH_3AuSH arising from an Au(s,p)→S transition corresponds to the 414-nm phosphorescent emission of $[(AuPH_3)_2$(i-mnt)] from Au−Au[$(sp)_\sigma$]→i-mnt charge transfer. Apparently, there is no Au−Au aurophilicity in the mononuclear PH_3AuSH molecule, but the emissions of 332 nm for PH_3AuSH and 414 nm for $[(AuPH_3)_2$(i-mnt)] are both MLCT in nature. It is the Au−Au aurophilicity in $[(AuPH_3)_2$(i-mnt)] that results in a ca. 80 nm red shift relative to the emission of PH_3AuSH. Bruce and co-workers[22] have studied the relationship between the Au−Au aurophilicity and the spectrum of the excited state for *cis*- and *trans*-

$[Au_2X_2C_2H_2(PH_2)_2]$ (X = Cl, Br and I) using ab initio methods. The calculations indicated that the aurophilic interaction stabilizes the first singlet excited state in the *cis* complex and leads to a red shift in the spectrum of the *cis* isomers relative to the *trans* isomers.

The intense 462-nm emission of the $[(AuPPh_3)_2$(i-mnt)] complex observed in the solid state at 20 K, and experimentally attributed to an Au→i-mnt charge transfer (^{3}MLCT),[33] agrees with our assignment for the 414-nm emission of $[(AuPH_3)_2$(i-mnt)]. The 50 nm difference between calculated and experimental emission wavelength may be because the single $[(AuPH_3)_2$(i-mnt)] molecule is not accurate enough to describe the solid-state emission of the $[(AuPPh_3)_2$(i-mnt)] complex at 20 K.

Recent studies on dinuclear $[AuS_2PR(OR)]_2$ (R = alkyl or aryl) complexes with MLCT excited-state properties have shown, by determining emissions of the Au^I complexes at different temperature (298 and 77 K), that the intermolecular Au−Au interaction in the solid state causes a red shift in emissive wavelengths.[14,15] The Au^I complexes were divided into two types: one, containing intermolecular Au−Au interactions in the solid state, has one emission at 298 K and two emissions at 77 K; and the other, without the intermolecular interaction in the solid, has no emissive band at 298 K but one band at 77 K. Apparently, the $[(AuPPh_3)_2$(i-mnt)] complex belongs to the second type because X-ray crystal-diffraction studies showed that it has no intermolecular Au−Au interaction in the solid state (shortest Au−Au of ca. 8.1 Å) and it possesses one emission of 462 nm in the solid state at 20 K.[33,41] Since the Au−Au separation is strongly related to the temperature,[14,15] there may be intermolecular Au−Au interactions between two adjacent $[(AuPPh_3)_2$(i-mnt)] molecules at 20 K. Therefore, the red shift of 50 nm for the solid-state emission at 20 K relative to the calculation can be rationalized by shortening the intermolecular Au−Au separations in the crystal lattice, which results in a lower-energy ^{3}MMLCT emission.

Since an intermolecular Au−Au interaction would affect the solid-state emission, we chose $[(AuPH_3)_2$(i-mnt)$]_2$ to simulate the solid-state luminescent properties of the Au^I complex at 20 K. The intermolecular Au−Au separation changes from 10.0 to 3.5 Å on keeping four Au atoms collinear and considering the least steric hindrance; the calculated emission wavelength varies from 412 to 450 nm. This shows that the intermolecular Au−Au interaction between two adjacent $[(AuPH_3)_2$(i-mnt)] molecules causes a ca. 40-nm red shift in the emission spectrum, which agrees with Fackler's studies mentioned above.[14,15] As the repeating unit of $[(AuPH_3)_2$(i-mnt)] increases it tends to the case of $[(AuPH_3)_2$(i-mnt)] in the solid state. Accordingly, the number of the intermolecular Au−Au interaction in the solid state at 20 K increases and the emission is anticipated to show a larger red shift. In fact, for MMLCT or MLCT transitions the Au−Au interactions have a systematic influence on the energies of the frontier orbitals responsible for the emission. The increasing number of intermolecular interactions in the solid state causes a net decrease of HOMO−LUMO energy gap. Therefore, the calculated 450-nm emission of $[(AuPH_3)_2$(i-mnt)$]_2$ agrees with the experimental 462-nm emission of the $[(AuPPh_3)_2$(i-mnt)] complex in the solid state at 20 K, and both have ^{3}MMLCT character.

The spectroscopic properties of $[(AuPH_3)_2$(i-mnt)] in the CH_2Cl_2 solution corresponding to the b^3A' excited state were also obtained by the CIS/IPCM methods. The calculated 333-nm emission arises from an ^{3}MLCT transition from the triplet excited state to the ground state, which blue-shifts ca. 120 nm relative to the 450-nm emission in the solid state. No emission has been found experimentally in the visible region for the $[(AuPPh_3)_2$(i-mnt)] complex in CH_2Cl_2 solution.[33,34]

Comparison of the calculated solid-state emissions with experiment shows that the single molecule $[(AuPH_3)_2$(i-mnt)] model is satisfactory for the ^{3}ILCT excited state (a^3A'). Because the intermolecular Au−Au interaction between two adjacent $[(AuPH_3)_2$(i-mnt)] molecules has almost no effect on the ^{3}ILCT excited state, the 593-nm phosphorescence corresponding to the excited state (Table 3) agrees well with the 595-nm emission of K_2(i-mnt) in the solid state at 20 K. However, the two-molecule $[(AuPH_3)_2$(i-mnt)$]_2$ model is required to rationalize the ^{3}MMLCT excited state as this excited state is strongly related to intermolecular Au−Au interactions. In the excited state, both intra- and intermolecular Au−Au interactions dramatically affect the solid-state emission, which ranges from 332 nm for mononuclear PH_3AuSH to 414 nm for dinuclear $[(AuPH_3)_2$(i-mnt)] to 450 nm for polynuclear $[(AuPH_3)_2$(i-mnt)$]_2$. Thus, the 450 nm phosphorescence of $[(AuPH_3)_2$(i-mnt)$]_2$ corresponds to the 462-nm emission of the $[(AuPPh_3)_2$(i-mnt)] complex in the solid state at 20 K, and both

Table 6. Excited state, corresponding Au−Au distance, emission wavelength and property of the excited state for $[Au_2(dpm)_2]^{2+}$, $[(AuPH_3)_2$(i-mnt)] and $[Au_2$(dpm)(i-mnt)]

	$[Au_2(dpm)_2]^{2+}$	$[(AuPH_3)_2$(i-mnt)]	$[Au_2$(dpm)(i-mnt)]
Excited state	^3A_u	$^3A'$	$^3A''$
Au−Au [Å]	2.74	2.95	3.39
Wavelength [nm]	331	414	411
Excited-state property	MCCT	MMLCT[a]	ILCT (MLCT)[a] [b]

[a] For MMLCT and ILCT (MLCT), L refers to i-mnt ligand. [b] Excited-state property of $[Au_2$(dpm)(i-mnt)] is i-mnt ILCT, modified by MLCT.

are ^{3}MMLCT in nature (triplet excited state to the ground state).

D. Comparison of the Luminescent Properties of $[Au_2(dpm)_2]^{2+}$, $[(AuPH_3)_2(i\text{-}mnt)]$ and $[Au_2(dpm)(i\text{-}mnt)]$

To reveal the luminescence regularity of the dinuclear Au^I complexes with the interchange of phosphane ligand and thiolate ligand, the calculated excited-state properties of $[Au_2(dpm)_2]^{2+}$,[28] $[(AuPH_3)_2(i\text{-}mnt)]$ and $[Au_2(dpm)(i\text{-}mnt)]$[58] are presented in Table 6. The phosphane ligand has little participation in the luminescence while the thiolate ligand is greatly involved in the transition. The excited-state properties of $[Au_2(dpm)_2]^{2+}$, $[(AuPH_3)_2(i\text{-}mnt)]$ and $[Au_2(dpm)(i\text{-}mnt)]$ change from MCCT to MMLCT to ILCT (MLCT), and the corresponding Au−Au distances vary from 2.74 to 2.95 to 3.39 Å. For $[Au_2(dpm)_2]^{2+}$ and $[(AuPH_3)_2(i\text{-}mnt)]$, the promotion of an electron from the antibonding orbitals to the s_σ and/or p_σ bonding orbitals of Au atoms results in an Au−Au σ-bond between the two Au atoms in the excited state; however, the charge transfer only occurs inside the i-mnt ligand and the metal simply modifies the i-mnt ILCT in the emission corresponding to the $^3A''$ excited state of the $[Au_2(dpm)(i\text{-}mnt)]$ complex. The stronger Au−Au aurophilicity causes the greater Au contribution to the transition, favoring an MCCT emissive excited state such as $[Au_2(dpm)_2]^{2+}$. Conversely, the excited state with the weaker Au−Au aurophilicity has less metal contribution and tends to be ILCT in character, such as $[Au_2(dpm)(i\text{-}mnt)]$.

In brief, ab initio investigations on $[Au_2(dpm)_2]^{2+}$, $[(AuPH_3)_2(i\text{-}mnt)]$ and $[Au_2(dpm)(i\text{-}mnt)]$ indicate that the Au−Au aurophilicity has no clear correlation with the emission wavelength but with the excited-state property. With the interchange of phosphane and thiolate ligands, the excited-state properties of such Au^I complexes regularly change from MCCT to MMLCT to ILCT.

Conclusions

The luminescence and Au−Au aurophilicity of $[(AuPH_3)_2(i\text{-}mnt)]$ in both the solid state and CH_2Cl_2 solution have been studied by ab initio methods. For the solid state, $[(AuPH_3)_2(i\text{-}mnt)]$ and $[(AuPH_3)_2(i\text{-}mnt)]_2$ models were employed to describe the spectroscopic properties. The former has been used to accurately calculate the ^{3}ILCT emissive excited state, because the intermolecular Au−Au interaction between the two adjacent $[(AuPH_3)_2(i\text{-}mnt)]$ molecules plays a minor role in the excited state. However, the ^{3}MMLCT emissive excited state is strongly related to the intermolecular Au−Au interaction between the two neighboring $[(AuPH_3)_2(i\text{-}mnt)]$ molecules in the solid state, especially at lower temperatures (20 K). The two-molecular model, $[(AuPH_3)_2(i\text{-}mnt)]_2$, can satisfactorily rationalize the solid-state emission of the $[(AuPPh_3)_2(i\text{-}mnt)]$ complex at 20 K. For dilute CH_2Cl_2 solutions, we used the single $[(AuPH_3)_2(i\text{-}mnt)]$ molecule associated with the IPCM in the SCRF method to calculate the absorption and emission. Most calculated spectra in solution agree with the experimental results.[33]

Studies on $[Au_2(dpm)_2]^{2+}$,[28] $[(AuPH_3)_2(i\text{-}mnt)]$ and $[Au_2(dpm)(i\text{-}mnt)]$ [58] show that the Au−Au aurophilicity is clearly correlated with the excited-state properties. With the interchange of phosphane and thiolate ligands, the excited-state properties of such Au^I complexes regularly change from MCCT to MMLCT to ILCT.

Acknowledgments

This work was supported by the Natural Science Foundation of China (20173021).

[1] [1a] R. L. White-Morris, M. M. Olmstead, F. Jiang, D. S. Tinti, A. L. Balch, *J. Am. Chem. Soc.* **2002**, *124*, 2327. [1b] R. L. White-Morris, M. M. Olmstead, A. L. Balch, *J. Am. Chem. Soc.* **2003**, *125*, 1033. [1c] R. L. White-Morris, M. M. Olmstead, F. Jiang, D. S. Tinti, A. L. Balch, *Inorg. Chem.* **2002**, *41*, 2313. [1d] M. M. Olmstead, F. Jiang, S. Attar, A. L. Balch, *J. Am. Chem. Soc.* **2001**, *123*, 3260. [1e] J. C. Vickery, M. M. Lomstead, E. Y. Fung, A. L. Balch, *Angew. Chem. Int. Ed. Engl.* **1997**, *36*, 1179.
[2] R. E. Bachman, S. A. Bodolosky-Bettis, S. C. Glennon, S. A. Sirchio, *J. Am. Chem. Soc.* **2000**, *122*, 7146.
[3] V. W.-W. Yam, E. C.-C. Cheng, *Angew. Chem. Int. Ed.* **2000**, *39*, 4240.
[4] M. Bardají, A. Laguna, V. M. Orera, M. D. Villacampa, *Inorg. Chem.* **1998**, *37*, 5125.
[5] J. M. Forward, Z. Assefa, J. P. Facker, Jr., *J. Am. Chem. Soc.* **1995**, *177*, 9103.
[6] Md. N. I. Khan, C. King, D. D. Heinrich, J. P. Fackler, Jr., L. C. Porter, *Inorg. Chem.* **1989**, *28*, 2150.
[7] B. Trzcinska-Bancroft, Md. N. I. Khan, J. P. Fackler, Jr., *Organometallics* **1988**, *7*, 993.
[8] S. Wang, G. Garzón, C. King, J.-C. Wang, J. P. Fackler, Jr., *Inorg. Chem.* **1989**, *28*, 4623.
[9] S. K. Chastain, W. R. Mason, *Inorg. Chem.* **1982**, *21*, 3717.
[10] J. Kozelka, H. R. Oswald, E. Dubler, *Acta Crystallogr., Sect. C* **1986**, *42*, 1007.
[11] J. M. Forward, D. Bohmann, J. P. Fackler, Jr., R. J. Staples, *Inorg. Chem.* **1995**, *34*, 6330.
[12] Y.-A. Lee, J. E. McGarrah, R. J. Lachicotte, R. Eisenberg, *J. Am. Chem. Soc.* **2002**, *124*, 10662.
[13] M. A. Mansour, W. B. Connick, R. J. Lachicotte, H. J. Gysling, R. Eisenberg, *J. Am. Chem. Soc.* **1998**, *120*, 1329.
[14] W. E. van Zyl, J. M. López-de-Luzuriaga, A. A. Mohamed, R. J. Staples, J. P. Fackler, Jr., *Inorg. Chem.* **2002**, *41*, 4579.
[15] W. E. van Zyl, J. M. López-de-Luzuriaga, J. P. Fackler, Jr., *J. Mol. Struct.* **2000**, *516*, 99.
[16] E. J. Fernández, C. Gimeno, A. Laguna, J. M. López-de-Luzuriaga, M. Monge, P. Pyykkö, D. Sundholm, *J. Am. Chem. Soc.* **2000**, *122*, 7287.
[17] S. S. Tang, C. P. Chang, I. J. B. Lin, L. S. Liou, J. C. Wang, *Inorg. Chem.* **1997**, *36*, 2294.
[18] V. W.-W. Yam, C.-K. Li, C.-L. Chan, *Angew. Chem. Int. Ed.* **1998**, *37*, 2857.
[19] H. Schmidbaur, *Gold Bull.* **1990**, *23*, 11.
[20] S. S. Pathaneni, G. R. Desiraju, *J. Chem. Soc., Dalton Trans.* **1993**, 319.
[21] M. A. Rawashdeh-Omary, M. A. Omary, H. H. Patterson, J. P. Fackler, Jr., *J. Am. Chem. Soc.* **2001**, *123*, 11237.
[22] P. Schwerdtfeger, A. E. Bruce, M. R. M. Bruce, *J. Am. Chem. Soc.* **1998**, *120*, 6587.
[23] [23a] P. Pyykkö, N. Runeberg, F. Mendizabal, *Chem. Eur. J.* **1997**, *3*, 1451. [23b] P. Pyykkö, F. Mendizabal, *Chem. Eur. J.* **1997**, *3*, 1458. [23c] P. Pyykkö, F. Mendizabal, *Inorg. Chem.* **1998**, *37*, 3018. [23d] P. Pyykkö, *Chem. Rev.* **1997**, *97*, 597. [23e]

P. Pyykkö, Y.-F. Zhao, *Angw. Chem.* **1991**, *103*, 622; *Angew. Chem. Int. Ed. Engl.* **1991**, *30*, 604. [23f] J. Li, P. Pyykkö, *Chem. Phys. Lett.* **1992**, *197*, 586. [23g] J. Li, P. Pyykkö, *Inorg. Chem.* **1993**, *32*, 2630.
[24] V. -W. W. Yam, K. K. W. Lo, *Chem. Soc. Rev.* **1999**, *28*, 323.
[25] S. Watase, M. Nakamoto, T. Kitamura, N. Kanehisa, Y. Kai, *J. Chem. Soc., Dalton Trans.* **2000**, 3585.
[26] C. King, J. C. Wang, M. N. I. Khan, J. P. Fackler, Jr., *Inorg. Chem.* **1989**, *28*, 2145.
[27] [27a] W.-F. Fu, K.-C. Chan, V. M. Miskowski, C.-M. Che, *Angew. Chem. Int. Ed.* **1999**, *38*, 2783. [27b] K. H. Leung, D. L. Phillips, M.-C. Tse, C.-M. Che, V. M. Miskowski, *J. Am. Chem. Soc.* **1999**, *121*, 4799. [27c] C.-M. Che, H.-L. Kwong, V. W.-W. Yam, K.-C. Cho, *J. Chem. Soc., Chem. Commun.* **1989**, 885. [27d] C.-M. Che, H.-L. Kwong, C.-K. Poon, *J. Chem. Soc., Dalton Trans.* **1990**, 3215.
[28] H.-X. Zhang, C.-M. Che, *Chem. Eur. J.* **2001**, *7*, 4887.
[29] C. D. Kim, S. Pillet, G. Wu, W. K. Fullagar, P. Coppens, *Acta Crystallogr., Sect. A* **2002**, *58*, 133.
[30] I. V. Novozhilova, A. V. Volkov, P. Coppens, *J. Am. Chem. Soc.* **2003**, *125*, 1079.
[31] R. Narayanaswamy, M. A. Young, E. Parkhurst, M. Ouellette, M. E. Kerr, K. M. Ho, R. C. Elder, A. E. Bruce, M. R. M. Bruce, *Inorg. Chem.* **1993**, *32*, 2506.
[32] W. B. Jones, J. Yuan, R. Narayanaswamy, M. A. Young, R. C. Elder, A. E. Bruce, M. R. M. Bruce, *Inorg. Chem.* **1995**, *34*, 1996.
[33] S. D. Hanna, J. I. Zink, *Inorg. Chem.* **1996**, *35*, 297.
[34] S. D. Hanna, S. I. Khan, J. I. Zink, *Inorg. Chem.* **1996**, *35*, 5813.
[35] M. Bardají, A. Laguna, P. G. Jones, A. K. Fischer, *Inorg. Chem.* **2000**, *39*, 3560.
[36] M. Bardají, A. Laguna, J. Vicente, *Inorg. Chem.* **2001**, *40*, 2675.
[37] V. -W. W. Yam, E. C. -C. Cheng, Z. -Y. Zhou, *Angew. Chem. Int. Ed.* **2000**, *39*, 1683.
[38] E. J. Fernández, J. M. López-de-Luzuriaga, M. Monge, M. A. Rodríguez, O. Crespo, M. C. Gimeno, A. Laguna, P. G. Jones, *Chem. Eur. J.* **2000**, *6*, 636.
[39] E. J. Fernández, J. M. López-de-Luzuraga, M. Monge, M. A. Rodríguez, O. Crespo, M. C. Gimeno, A. Laguna, P. G. Jones, *Inorg. Chem.* **1998**, *37*, 6002.
[40] O. Crespo, A. Laguna, E. J. Fernández, J. M. López-de-Luzuriaga, P. G. Jones, M. Teichert, M. Monge, P. Pyykkö, N. Runeberg, M. Schütz, H. -J. Werner, *Inorg. Chem.* **2000**, *39*, 4786.
[41] M. N. I. Khan, S. Wang, D. D. Heinrich, J. P. Fackler, Jr., *Acta Crystallogr., Sect. C* **1998**, *44*, 822.
[42] [42a] M. J. McKeage, L. Maharaj, S. J. Berners-Price, *Coord. Chem. Rev.* **2002**, *232*, 127. [42b] S. J. Berners-Price, G. R. Girard, D. T. Hill, B. M. Sutton, P. S. Jarrett, L. F. Faucette, R. K. Johnson, C. K. Mirabelli, P. J. Sadler, *J. Med. Chem.* **1990**, *33*, 1386. [42c] E. J. Corey, M. M. Mahrotra, A. U. Khan, *Science* **1987**, *236*, 68. [42d] C. K. Mirabelli, R. K. Johnson, D. T. Hill, L. F. Faucette, G. R. Girard, G. Y. Kuo, C. M. Sung, S. T. Crooke, *J. Med. Chem.* **1986**, *29*, 218. [42e] J. Weinstock, B. M. Sutton, G. Y. Kuo, D. T. Walz, M. J. Dimartino, *J. Med. Chem.* **1974**, *17*, 139. [42f] C. F. Shaw, III, A. Beery, *Inorg. Chim. Acta* **1986**, *123*, 213.
[43] L. Hao, R. J. Lachicotte, H. J. Gysling, R. Eisenberg, *Inorg. Chem.* **1999**, *38*, 4616.
[44] M. O. Wolf, M. A. Fox, *J. Am. Chem. Soc.* **1995**, *117*, 1845.
[45] O. D. Häberlen, N. Rösch, *J. Phys. Chem.* **1993**, *97*, 4970.
[46] E. J. Fernández, M. C. Gimeno, P. G. Jones, A. Laguna, M. Laguna, J. M. López-de-Luzuriaga, M. A. Rodriguez, *Chem. Ber.* **1995**, *128*, 121.
[47] B. I. Dunlap, N. Rösch, *Adv. Quantum Chem.* **1990**, *21*, 317.
[48] C. Møller, M. S. Plesset, *Phys. Rev.* **1934**, *46*, 618.
[49] [49a] J. B. Foresman, M. Head-Gordon, J. A. Pople, M. J. Frisch, *J. Phys. Chem.* **1992**, *96*, 135. [49b] K. Raghavachari, J. A. Pople, *Int. J. Quant. Chem.* **1981**, *20*, 167.
[50] J. B. Foresman, T. A. Keith, K. B. Wiberg, J. Snoonian, M. J. Frisch, *J. Phys. Chem.* **1996**, *100*, 16098.
[51] L. E. Sanscores, R. Salcedo, H. Flores, A. Martinez, *J. Mol. Struct. (TheoChem)* **2000**, *530*, 125.
[52] J. B. Foresman, A. Frisch, *Exploring Chemistry with Electronic Structure Method*, Gaussian, Inc., Pittsburgh, PA **1996**.
[53] M. J. Frisch, G. W. Trucks, H. B. Schlegel, G. E. Scuseria, M. A. Robb, J. R. Cheeseman, V. G. Zakrzewski, J. A. Montgomery, Jr., R. E. Stratmann, J. C. Burant, S. Dapprich, J. M. Millam, A. D. Daniels, K. N. Kudin, M. C. Strain, O. Farkas, J. Tomasi, V. Barone, M. Cossi, R. Cammi, B. Mennucci, C. Pomelli, C. Adamo, S. Clifford, J. Ochterski, G. A. Petersson, P. Y. Ayala, Q. Cui, K. Morokuma, D. K. Malick, A. D. Rabuck, K. Raghavachari, J. B. Foresman, J. Cioslowski, J. V. Ortiz, A. G. Baboul, B. B. Stefanov, G. Liu, A. Liashenko, P. Piskorz, I. Komaromi, R. Gomperts, R. L. Martin, D. J. Fox, T. Keith, M. A. Al-Laham, C. Y. Peng, A. Nanayakkara, M. Challacombe, P. M. W. Gill, B. Johnson, W. Chen, M. W. Wong, J. L. Andres, C. Gonzalez, M. Head-Gordon, E. S. Replogle, and J. A. Pople, *Gaussian 98, Revision A.9*, Gaussian, Inc., Pittsburgh PA, **1998**.
[54] [54a] W. R. Wadt, P. J. Hay, *J. Chem. Phys.* **1985**, *82*, 284. [54b] P. J. Hay, W. R. Wadt, *J. Chem. Phys.* **1985**, *82*, 299.
[55] D. Perreault, M. Drouin, A. Michel, V. M. Miskowski, W. P. Schaefer, P. D. Harvey, *Inorg. Chem.* **1992**, *31*, 695.
[56] A. Bondi, *J. Phys. Chem.* **1964**, *68*, 441.
[57] B. G. Werden, E. Billig, H. B. Gray, *Inorg. Chem.* **1966**, *5*, 78.
[58] Q.-J. Pan, H. -X. Zhang, submitted to *J. Phys. Chem.*

Received June 23, 2003
Early View Article
Published Online October 2, 2003

